ACI JOURNAL TECHNICAL PAPER

Title no. 81-26

# Deformation of Progressively Cracking Reinforced Concrete Beams

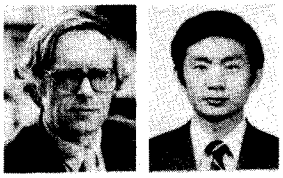

by Zdeněk P. Bažant and Byung H. Oh

*A consistent theory for the analysis of curvature and deflections of reinforced concrete beams in the cracking stage is presented. The theory assumes concrete to have a nonzero tensile carrying capacity, characterized by a uniaxial stress-strain diagram which characterizes progressive microcracking due to strain softening. The tensile stress-strain properties are the same as those which are obtained in direct tensile tests and those which have recently been used with success in modeling fracture test results for concrete. The theory agrees well with the simpler formula of Branson within the range for which his formula is intended. The value of the proposed theory is its much broader applicability. Aside from demonstrating a good agreement with available test data for short-time deformations up to the ultimate load, it is shown that the theory also correctly predicts the longtime creep deformations of cracked beams. To this end, the average creep coefficient for tensile response including peak stress and strain softening needs to be taken about three times larger than that for compression states. The theory also predicts the reduction of creep deflections achieved by the use of compression reinforcement, and a comparison of modeling this effect is made with an ACI formula. As a simplified version of the model, it is proposed to replace the tensile strain-softening behavior by the use of an equivalent tensile area of concrete at the level of tensile steel, behaving linearly. Assuming this area to be a constant, realistic predictions for short-time as well as longtime deformations in the service stress range can still be obtained.*

**Keywords: beams (supports);** bending; **cracking (fracturing);** creep properties; deflection; **deformation; reinforced concrete;** structural analysis; tensile properties.

The bending stiffness of unprestressed or partially prestressed reinforced concrete beams under service loads is considerably smaller than the stiffness calculated on the basis of uncracked cross sections. This is because the beam contains numerous tensile cracks. Yet, at the same time, the stiffness is significantly higher than that calculated when the tensile resistance of concrete is neglected. This phenomenon, often termed tension stiffening, is attributed to the fact that concrete does not crack suddenly and completely but undergoes progressive microcracking (strain softening).

Based on numerous tests,[1-7] Branson[1,3,4,8] derived an empirical formula which adequately describes the test results and has been endorsed by an ACI committee.[1] Whereas this formula well serves practical purposes, it is not derived from the intrinsic material properties of concrete, particularly the strain-softening properties. This paper will develop a realistic model which is derived from such properties. Although a great improvement over Branson's formula predictions for the curvature and deflection of reinforced concrete beams under short-time loading can hardly be expected, our effort leads to other important advantages. If the model is derived from the basic material properties, which are the same as those that work in other situations where progressive microcracking plays a role, such as fracture mechanics of concrete, the applicability of the model should be broader than that of Branson's formula. The model should predict curvatures and deflections beyond the service stress range all the way to the ultimate load and beyond and should also be applicable to long-time loading when creep is taken into account, or flexure at axial compression, bending of slabs and thin shells, deformations of deep beams and thick shells, deformation due to diagonal shear or torsion, etc. Among these possible generalizations which can be contemplated when a theory based on material properties is used, we will demonstrate here the first two and will try to substantiate these generalizations by comparisons with available test data. In short, it is not our intention to supersede Branson's formula but to develop a model of a more general validity. This will, of course, be at some cost to simplicity.

## CALCULATION OF CURVATURE AND DEFLECTION USING TENSILE STRAIN-SOFTENING DIAGRAM

Tests in extremely stiff testing machines have clearly demonstrated[9-13] that concrete exhibits tensile strain-

Received November 19, 1982, and reviewed under Institute publication policies.  Pertinent discussion will be published in the March-April 1985 JOURNAL if received by Dec. 1, 1984.

*Zdeněk P. Bažant, FACI, is a professor and director, Center for Concrete and Geomaterials, Northwestern University. Dr. Bažant is a registered structural engineer, serves as consultant to Argonne National Laboratory and several other firms, and is on editorial boards of five journals. He serves as chairman of RILEM Committee TC69 on creep, of ASCE-EMD Committee on Properties of Materials, and of IA-SMiRT Division H. His works on concrete and geomaterials, inelastic behavior, fracture, and stability have been recognized by a RILEM medal, ASCE Huber Prize and T. Y. Lin Award, IR-100 Award, Guggenheim Fellowship, Ford Foundation Fellowship, and election as Fellow of American Academy of Mechanics.*

***Byung H. Oh** is an assistant professor of civil engineering at the Seoul National University, Korea. He received his PhD from Northwestern University in 1982. Prior to joining Seoul National University, Dr. Oh was a visiting research engineer at the Research Laboratory of the Portland Cement Association, Skokie, Ill. His research interests include concrete and reinforced concrete, inelastic behavior, fracture, cracking, constitutive relations, and mathematical modeling.*

softening, i.e., a gradual decline of tensile stress with increasing strain [Fig. 1(b)]. This behavior may be approximated, for the present purposes, by a bilinear stress-strain diagram characterized as follows [Fig. 1(a)]

$$\text{For } \epsilon_c \leqslant \epsilon_{tp}; \qquad \sigma_c = E_c\epsilon_c \tag{1}$$

$$\text{For } \epsilon_{tp} < \epsilon_c < \epsilon_{tf}; \quad \sigma_c = f_t' - (\epsilon_c - \epsilon_{tp})(-E_t) \tag{2}$$

$$\text{For } \epsilon_c > \epsilon_{tf}; \qquad \sigma_c = 0 \tag{3}$$

in which $\sigma_c$, $\epsilon_c$ = uniaxial stress and strain of concrete, $E_c$ = Young's elastic modulus of concrete, $f_t'$ = direct tensile strength, $E_t$ = tangent strain-softening modulus [negative, Fig. 1(a)], $\epsilon_{tp}$ = strain at peak tensile stress, and $\epsilon_{tf}$ = final strain when the tensile stress is reduced to zero [full fracture, Fig. 1(a)]. A stepwise stress-strain diagram which is approximately equivalent to Eq. (1) through (3) has been used by Scanlon[14] and by Scordelis and co-workers.[15] Recently it was discovered that Eq. (1) through (3), combined with a fracture mechanics energy concept, are capable of consistently describing all essential fracture test data for concrete.[2] This study, in turn, greatly increased the data base relevant, albeit indirectly, to tensile strain-softening, which further allowed setting up a realistic prediction formula[2] for $E_t$

$$E_t = \frac{-70\,E_c}{57 + f_t'} \tag{4}$$

in which $E_c$, $f_t'$, and $E_t$ are in psi (psi = 6895 Pa).

For concrete in uniaxial compression, a well-known expression for the stress-strain relation covering the compression strain-softening is used[16] [Fig. 1(b)]

$$\sigma_c = \frac{E_c\epsilon_c}{1 + \left(\frac{E_c\epsilon_{cp}}{\sigma_{cp}} - 2\right)\left(\frac{\epsilon_c}{\epsilon_{cp}}\right) + \left(\frac{\epsilon_c}{\epsilon_{cp}}\right)^2} \tag{5}$$

in which $\sigma_{cp}$ = peak stress (compression strength $f_c'$), and $\epsilon_{cp}$ = strain at peak stress, both in compression. The steel is assumed as elastic-perfectly plastic, characterized by Young's elastic modulus $E_s$ and uniaxial yield stress $f_y$. Work hardening at large plastic strain is not needed for the calculations which follow.

The usual Bernoulli-Navier's hypothesis that plane cross sections of the beam remain plane and orthogonal is adopted. Further, it is assumed that the average strain in steel equals the average strain in concrete at the same level, i.e., the overall bond slip is zero (alternating local bond slips between cracks are not inconsistent with this assumption). The analysis of the rectangular cross section shown in Fig. 1(d) is now routine. The cross section areas of compression and tension reinforcement are $A_{s1}$ and $A_{s2}$, respectively, their strains are $\epsilon_{sj}$ ($j$ = 1, 2), their stresses are $\sigma_{sj}$, and their force

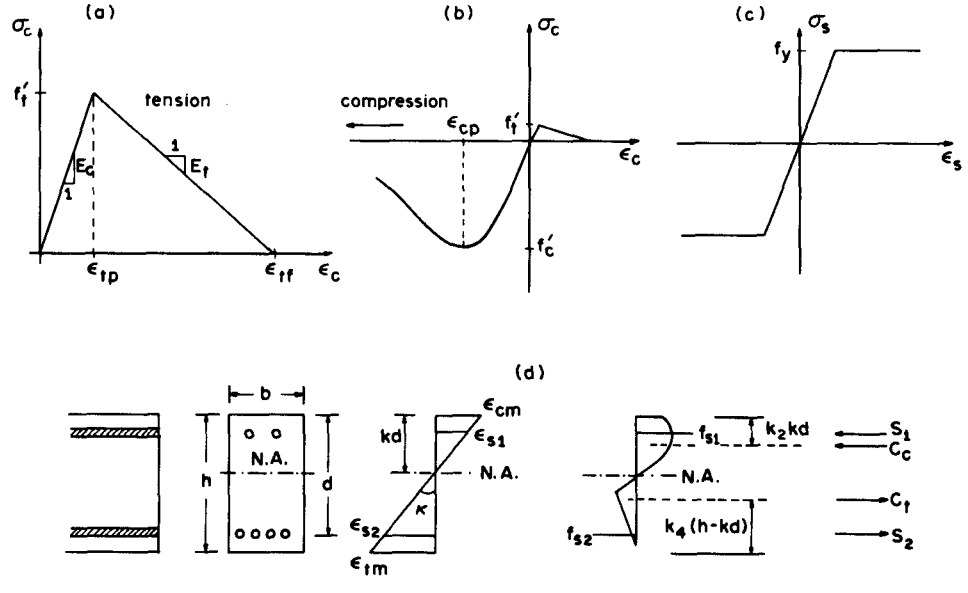


*Fig. 1 — Assumed uniaxial stress-strain relations for concrete in tension and compression (a, b) and for steel (c); and stress and strain distributions in the cross section of beams (d)*

resultants are $S_j = \sigma_{sj}A_{sj}$. For a given strain of concrete at the compression face $\epsilon_{cm}$ and a given depth $kd$ to neutral axis [where $d$ = depth to tensile reinforcement, Fig. 1(d)], the linearity of strain distribution requires that

$$\epsilon_{sj} = \epsilon_{cm}\frac{kd - d_j}{kd} \quad (j = 1, 2) \tag{6}$$

where the steel stresses $\sigma_{sj}$ follow from the stress-strain diagram of steel.

The resultant of compressive stresses in concrete may be expressed as

$$C_c = k_1 f_c' bkd \tag{7}$$

where parameter $k_1$ defines the average compressive stress, and $b$ = cross section width. This resultant acts at a distance $k_2kd$ below the compression face[35] [Fig. 1(d)]. Based on the given stress-strain diagram, one may write

$$k_1 = \frac{\int_0^{\epsilon_{cm}} \sigma_c d\epsilon_c}{f_t' \epsilon_{cm}}, \quad k_2 = 1 - \frac{\int_0^{\epsilon_{cm}} \epsilon_c \sigma_c d\epsilon_c}{\epsilon_{cm}\int_0^{\epsilon_{cm}} \sigma_c d\epsilon_c} \tag{8a,b}$$

Similarly, the resultant of tensile stresses in concrete (due to strain softening) and its distance from the tension face may be expressed as

$$C_t = k_3 f_t' b\,(h - kd), \quad z_1 = k_4\,(h - kd) \tag{9}$$

in which

$$k_3 = \frac{\int_0^{\epsilon_{tm}} \sigma_c d\epsilon_c}{f_t' \epsilon_{tm}}, \quad k_4 = 1 - \frac{\int_0^{\epsilon_{tm}} \epsilon_c \sigma_c d\epsilon_c}{\epsilon_{tm}\int_0^{\epsilon_{tm}} \sigma_c d\epsilon_c} \tag{10a,b}$$

Here $\epsilon_{tm} = \epsilon_{cm}(h - kd)/kd$ = concrete strain at tension face, and $h$ = beam depth.

By substituting Eq. (5) into Eq. (8a, b) one obtains

$$k_1 = \frac{E_c}{f_c' \epsilon_{cm}}\left[\frac{1}{2B}\ell n(1 + A\epsilon_{cm} + B\epsilon_{cm}^2) + \frac{A}{B\sqrt{q}}\left(\tan^{-1}\frac{A}{\sqrt{q}} - \tan^{-1}\frac{A + 2B\epsilon_{cm}}{\sqrt{q}}\right)\right] \tag{11}$$

$$k_2 = 1 - \left[\frac{\epsilon_{cm}}{B} - \frac{A}{2B^2}\ell n(1 + A\epsilon_{cm} + B\epsilon_{cm}^2) + \left(\frac{A^2 - 2B}{B^2\sqrt{q}}\right)\left(\tan^{-1}\frac{2B\epsilon_{cm} + A}{\sqrt{q}} - \tan^{-1}\frac{A}{\sqrt{q}}\right)\right] \div \epsilon_{cm}\left[\frac{1}{2B}\ell n(1 + A\epsilon_{cm} + B\epsilon_{cm}^2) + \frac{A}{B\sqrt{q}}\left(\tan^{-1}\frac{A}{\sqrt{q}} - \tan^{-1}\frac{2B\epsilon_{cm} + A}{\sqrt{q}}\right)\right] \tag{12}$$

in which

$$A = \frac{1}{\epsilon_{cp}}\left(\frac{E_c\epsilon_{cp}}{\sigma_{cp}} - 2\right), \quad B = \frac{1}{\epsilon_{cp}^2}, \quad q = 4B - A^2 > 0 \tag{13}$$

Substituting Eq. (1) through (3) into Eq. (10a,b), one further obtains for $\epsilon_{tm} \leqslant \epsilon_{tp}$

$$k_3 = \frac{E_c\epsilon_{tm}}{2f_t'}, \quad k_4 = \frac{1}{3} \tag{14}$$

for $\epsilon_{tp} < \epsilon_{tm} < \epsilon_{tf}$

$$k_3 = \frac{1}{f_t' \epsilon_{tm}}\left[(f_t' + \epsilon_{tp}|E_t|)\epsilon_{tm} - \frac{1}{2}|E_t|\epsilon_{tm}^2 - \frac{1}{2}f_t'\epsilon_{tp} - \frac{1}{2}|E_t|\epsilon_{tp}^2\right] \tag{15}$$

$$k_4 = 1 - \left[-\frac{1}{6}f_t'\epsilon_{tp}^2 + \left(\frac{1}{2}f_t' + \frac{1}{2}|E_t|\epsilon_{tp}\right)\epsilon_{tm}^2 - \frac{1}{3}|E_t|\epsilon_{tm}^3 - \frac{1}{6}|E_t|\epsilon_{tp}^3\right] \div \epsilon_{tm}\left[(f_t' + \epsilon_{tp}|E_t|)\epsilon_{tm} - \frac{1}{2}|E_t|\epsilon_{tm}^2 - \frac{1}{2}f_t'\epsilon_{tp} - \frac{1}{2}|E_t|\epsilon_{tp}^2\right] \tag{16}$$

for $\epsilon_{tm} \geqslant \epsilon_{tf}$

$$k_3 = \frac{1}{f_t' \epsilon_{tm}}\left[(f_t' + \epsilon_{tp}|E_t|)\epsilon_{tf} - \frac{1}{2}|E_t|\epsilon_{tf}^2 - \frac{1}{2}f_t'\epsilon_{tp} - \frac{1}{2}|E_t|\epsilon_{tp}^2\right] \tag{17}$$

$$k_4 = 1 - \left[-\frac{1}{6}f_t'\epsilon_{tp}^2 + \left(\frac{1}{2}f_t' + \frac{1}{2}|E_t|\epsilon_{tp}\right)\epsilon_{tf}^2 - \frac{1}{3}|E_t|\epsilon_{tf}^3 - \frac{1}{6}|E_t|\epsilon_{tp}^3\right] \div \epsilon_{tm}\left[(f_t' + \epsilon_{tp}|E_t|)\epsilon_{tf} - \frac{1}{2}|E_t|\epsilon_{tf}^2 - \frac{1}{2}f_t'\epsilon_{tp} - \frac{1}{2}|E_t|\epsilon_{tp}^2\right] \tag{18}$$

Now the force and moment equilibrium conditions may be written as

$$N = k_1 f_c' bkd + \sum_{j=1}^{2}\sigma_{sj}A_{sj} - k_3 f_t' b\,(h - kd) \tag{19}$$

$$M = k_1 f_c' bkd\left(\frac{h}{2} - k_2kd\right) + \sum_{i=1}^{2}\sigma_{si}A_{si}\left(\frac{h}{2} - d_i\right) + k_3 f_t' b\,(h - kd)\left[\frac{h}{2} - k_4(h - kd)\right] \tag{20}$$

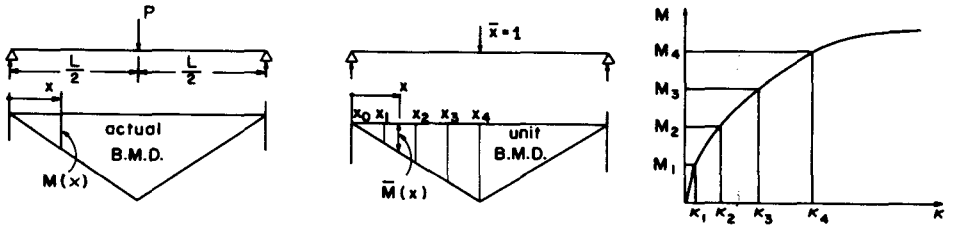


*Fig. 2 — Diagrams for evaluating deflections*

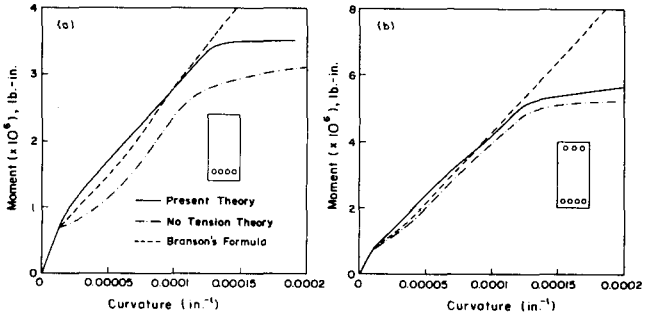


*Fig. 3 — Comparisons of present theory with Branson's formula for moment-curvature diagram and with no-tension theory*

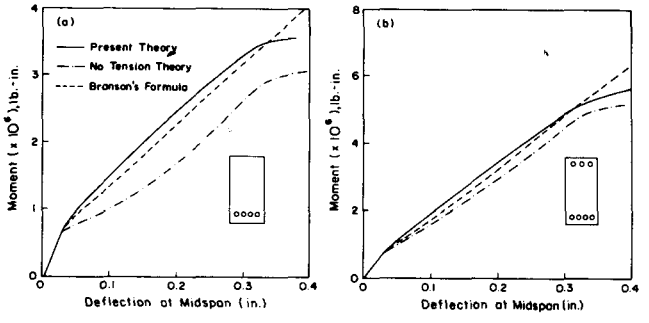


*Fig. 4 — Comparison of present theory with Branson's formula for moment-deflection curve and with no-tension theory*

in which $N$ and $M$ = normal force and bending moment in the cross section. Finally, the beam curvature is

$$\kappa = \frac{\epsilon_{cm}}{kd} \tag{21}$$

To calculate the moment-curvature relation for a given normal force $N$ (in our case $N = 0$), we may consider a succession of $\epsilon_{cm}$ values increasing in small increments. For each of them, we obtain depth $kd$ to the neutral axis from Eq. (19). The bending moment and curvature then follow from Eq. (20) and (21).

According to the principle of virtual work, deflection $\delta$ of the beam may be calculated as

$$\delta = \int_0^L \kappa \bar{M} dx \tag{22}$$

in which $\bar{M}$ = bending moment distribution corresponding to a unit load in the sense of deflection $\delta$. In numerical calculations the last integral has been evaluated numerically by Simpson's rule with four divisions for a half span of a simply supported beam of span $L$, with a concentrated load at midspan (for which $\bar{M} = x/2$)

$$\delta = 2\int_0^{L/2} \frac{x}{2}\kappa(x)dx \simeq \frac{L^2}{48}\left[\kappa\left(\frac{L}{8}\right) + \kappa\left(\frac{L}{4}\right) + 3\kappa\left(\frac{3L}{8}\right) + \kappa\left(\frac{L}{2}\right)\right] \tag{23}$$

Here the arguments of $\kappa$ represent the distances from beam support, and $\delta$ is the deflection at midspan (Fig. 2). The curvature values are here calculated from the moment-curvature relation obtained as already described. In this manner, individual points of the load-deflection diagram can be calculated.

## Numerical examples and comparisons with test data

For the sake of illustration, we present two numerical examples pertaining to both singly and doubly reinforced simply supported beams subjected to a concentrated load at midspan (Fig. 2), for which we calculate the moment-curvature diagram (Fig. 3) and the moment-deflection diagram (Fig. 4). The design parameters for the singly reinforced beam [Fig. 3(a) and Fig. 4(a)] are $b$ = 12 in., $h$ = 24 in., $A_s$ = 5 in.$^2$, $d$ = 20 in., $f_c'$ = 3600 psi, $f_t'$ = 450 psi, $E_c = 3.42 \times 10^6$ psi, $f_y$ = 40,000 psi, $E_s = 29 \times 10^6$ psi, and $L$ = 180 in. (where 1 in. = 25.4 mm, 1 psi = 6895 Pa). The design parameters for the doubly reinforced beam [Fig. 3(b) and Fig. 4(b)] are $b$ = 11 in., $h$ = 22.5 in., $A_s$ = 8.57 in.$^2$, $A_s'$ = 4.48 in.$^2$, $d'$ = 2.5 in., $d$ = 20 in., $f_c'$ = 3000 psi, $f_t'$ = 411 psi, $E_c = 3.12 \times 10^6$ psi, $f_y$ = 40,000 psi, and $E_s = 29 \times 10^6$ psi.

In Fig. 3 and 4, the solid lines represent the results from the present theory which takes into account the tensile stresses in concrete. For comparison, we also show the results of a calculation in which all assumptions are the same except that the tensile stresses in concrete are neglected; see the dash-dot lines. Furthermore, we also show for comparison the results obtained from Branson's formula based on his effective moment of inertia $I_e$;[3-6] see the dashed lines. As seen from these comparisons, the neglect of tensile capacity of concrete leads to a serious underestimation of stiffness in case of singly reinforced beams but a relatively

small underestimation in case of doubly reinforced beams. Further, we see that our theory agrees very well with Branson's formula previously verified by experiments. In addition, our theory also describes the range of steel yielding and compression nonlinearity of concrete for which Branson's formula was not intended. With regard to these comparisons one should stress again that the tensile stress-strain relation for concrete was the same as that determined by direct tension tests and subsequently also validated by comparison with fracture test data.

Our model can be compared with the test data in the literature from References 17 through 20. Comparisons of the predictions of our model with these data are shown in Fig. 5 through 7, and the material parameters corresponding to the curves shown are summarized in Table 1. The values of the three parameters needed in the model, $f'_c$, $E_c$ and $f'_t$, were taken as reported by the experimentalists; however, in the cases where no value of $E_c$ or $f'_t$ was reported, an estimate was made from $f'_c$ using the ACI formulas. Generally, the comparisons in Fig. 5 through 7 reveal a satisfactory agreement which validates the present model.

## Longtime beam deformations based on tensile strain-softening

Having validated a theory that is fully based on basic material properties (which are the same as those which suffice to predict fracture test results as well), we may consider whether the same theory also applies to creep deflections. Although for comparisons with existing test data the choice of the creep formulation is unimportant (since no deflection data of very long duration, very different ages at loading, different drying conditions, etc., seem to exist), we will choose the recently developed BP2 Model[21] which has been shown to agree reasonably well with numerous test data from the literature over a broad range of conditions. Adopting, as usual, the linear principle of superposition, the creep properties are fully characterized by the compliance function $J(t, t')$(also called the creep function), which represents the strain at age $t$ caused by a uniaxial unit stress acting since age $t'$. According to the BP2 Model

$$J(t,t') = \frac{1}{E_0} + C_0(t,t') + C_d(t,t',t_0) \qquad (24)$$

with

$$C_0(t,t') = \frac{\phi_1}{E_0}(t'^{-m} + \alpha)(t - t')^n$$

$$C_d(t,t',t_0) = \frac{\bar{\phi}_d}{E_0} k'_h t'^{-m/2} S_d(t,t') \qquad (25)$$

in which $E_0$ = asymptotic modulus; $C_0(t,t')$ = basic creep compliance; $C_d(t, t', t_0)$ = drying creep compliance; $m$, $n$, $\alpha$, $\phi_1$, $\phi_d$, $k'_h$ = material parameters; $t_0$ = age of concrete at the start of drying; and $S_d(t, t')$ = a shrinkage function involving the drying half-time which is proportional to the square of the size of cross section. In all present calculations, the parameter values predicted by the formulas in Reference 21 have been used (see Reference 21 for details). The value of the short-time elastic modulus $E(t')$ may be obtained from Eq. (24) and (25) as $E(t') = 1/J(t' + \Delta, t')$ in

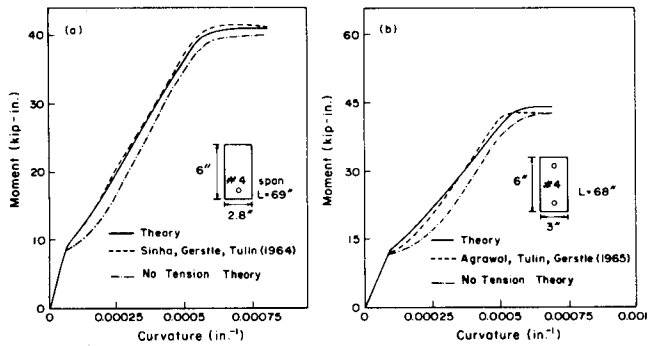


*Fig. 5 — Comparison of present theory with the tests by (a) Sinha, Gerstle, Tulin (1964); and (b) Agrawal, Tulin, Gerstle (1965)*

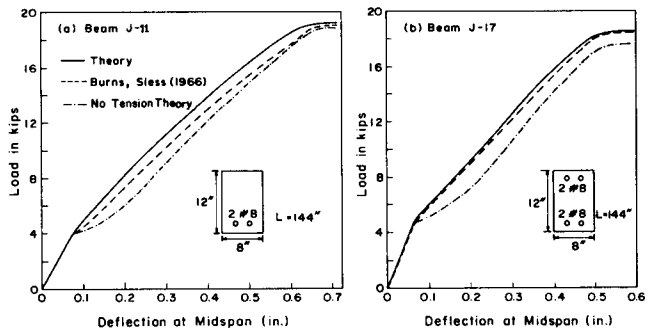


*Fig. 6 — Comparison of present theory with deflection tests by Burns and Siess (1966)*

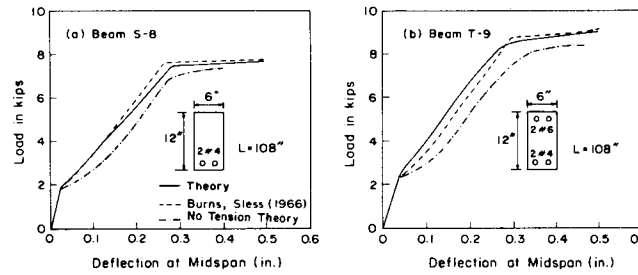


*Fig. 7 — Comparison of present theory with further deflection tests by Burns and Siess (1966)*

**Table 1 — Parameters for test data**

| Test series | $f'_c$, psi | $E_c$, ksi | $f'_t$, psi |
|---|---|---|---|
| Sinha, Gerstle, Tulin | 3750 | 3490* | 306* |
| Agrawal, Tulin, Gerstle | 4400 | 2100 | 332* |
| Burns, Siess | | | |
| Number 1 | 4110 | 3654* | 320* |
| Number 2 | 3900 | 3560* | 312* |
| Number 3 | 2640 | 2929* | 257* |
| Number 4 | 2690 | 2956* | 259* |
| Hollington | 5100 | 3000 | 495 |

1 psi = 6895 Pa, 1 ksi = 1000 psi.
*Asterisks indicate numbers estimated by calculations; without asterisk - as reported.

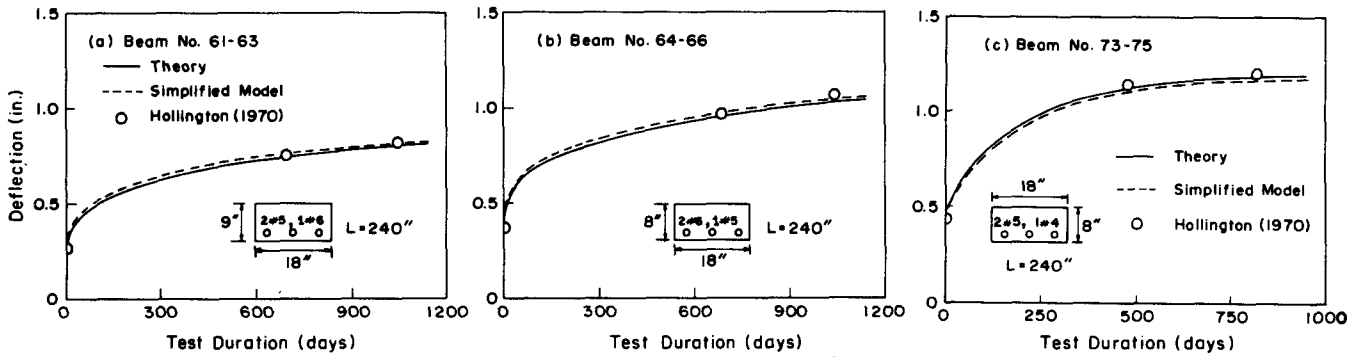


*Fig. 8 — Comparison of time-dependent creep deflection from present theory with Hollington's tests (1970)*

which $\Delta = 0.1$ day.[21] Determining $E(t')$ from $J(t,t')$ is important since other formulas for $E$ do not yield values which would be consistent with the creep coefficient $\phi(t,t')$. The latter's value may be calculated as

$$\phi(t,t') = E(t')J(t,t') - 1 \tag{26}$$

Although structural analysis can be carried out quite simply and more accurately by the age-adjusted effective modulus method[22-24] for the deformations of cracked reinforced concrete beams, almost equally good results can be obtained using the effective modulus method[3,22,25,26] (which is still simpler) provided the loading is constant in time. This method consists in carrying out, for the full applied loads, an elastic analysis based on the effective modulus

$$E_{eff} = \frac{E(t')}{1 + \phi(t,t')} = \frac{1}{J(t,t')} \tag{27}$$

If $E_c$ is replaced by $E_{eff}$, the foregoing analysis [Eq. (5) through (23)] becomes applicable also to longtime deformations.

The longtime deformation data with which the present model can be compared are those of Hollington[27] (Fig. 8). In comparisons with these data it has been found, not surprisingly, that for tensile stresses the creep coefficient must be considered larger than that for compression stresses as given by Eq. (24) through (26), approximately three times larger

$$[\phi(t,t')]_{\text{average, tension}} = 3\,[\phi(t,t')]_{\text{compression, Eq. (24) through (26)}} \tag{28}$$

Although there are no direct measurements to this effect, the conclusion is not surprising since in the strain-softening range concrete is known to creep much faster than in the initial linear strain range. The creep coefficient for tensile stresses less than about one-half of $f_t'$ is about the same as for compression. However, in the present model, the stresses near the peak stress $f_t'$ and the post-peak behavior matter; in that range, an increased creep is reasonable due to the progressive development of microcracks in time. Eq. (28) describes this phenomenon in the average sense for the entire tensile range.

Aside from Eq. (28), no other parameters have been adjusted to obtain optimum fits, and the solid lines in Fig. 8 represent the predictions exactly as obtained from the present theory using the creep prediction formulas from Reference 21. As seen from Fig. 8, the agreement with tests is again satisfactory. (This not only further validates our theory but also lends additional indirect support for the BP2 Model.) The reason why Fig. 8 is plotted in actual time rather than log-time is that the time range of the available data is limited.

With regard to creep deflections, another effect which is of considerable practical importance and has been studied experimentally is compression reinforcement. The use of such reinforcement is known to reduce the longtime deflections substantially.[28-30] In 1972, ACI Committee 435[1] recommended for the creep deflection of beams $\delta_{cp}$ the following formulas

$$\delta_{cp} = k_r \phi(t,t')\,\delta_i$$
$$k_r = 0.85 - 0.45A_s'/A_s \geqslant 0.40 \tag{29a}$$

and in 1978 this committee[3,31,32] revised $k_r$ as

$$k_r = 1/(1 + 50\,\rho') \tag{29b}$$

where $\rho' = A_s'/bd$ and $\delta_i$ = initial short-time deflection. For the creep coefficient, Subcommittee 2 of ACI 209[3-6,24] recommends the formulas developed by Branson et al.

$$C_t = \phi_u(t')\,f(t - t'),\ f(t - t')$$
$$= \frac{(t - t')^{0.6}}{10 + (t - t')^{0.6}},\ \phi_u(t') = \phi(\infty, 7)\ 1.25t'^{-0.118} \tag{30}$$

in which all times are given in days. Other, more complicated, formulas[21,33] give more realistic values over a broader range of times and various influencing factors, but for the present purposes the differences are unimportant.

The formulas in Eq. (29a, b), in conjunction with those in Eq. (30), have been validated experimentally.[3,5] Fig. 9 shows the comparison of the present theory with the results obtained from Eq. (29a,b) through (30) for several typical designs of simply supported beams.

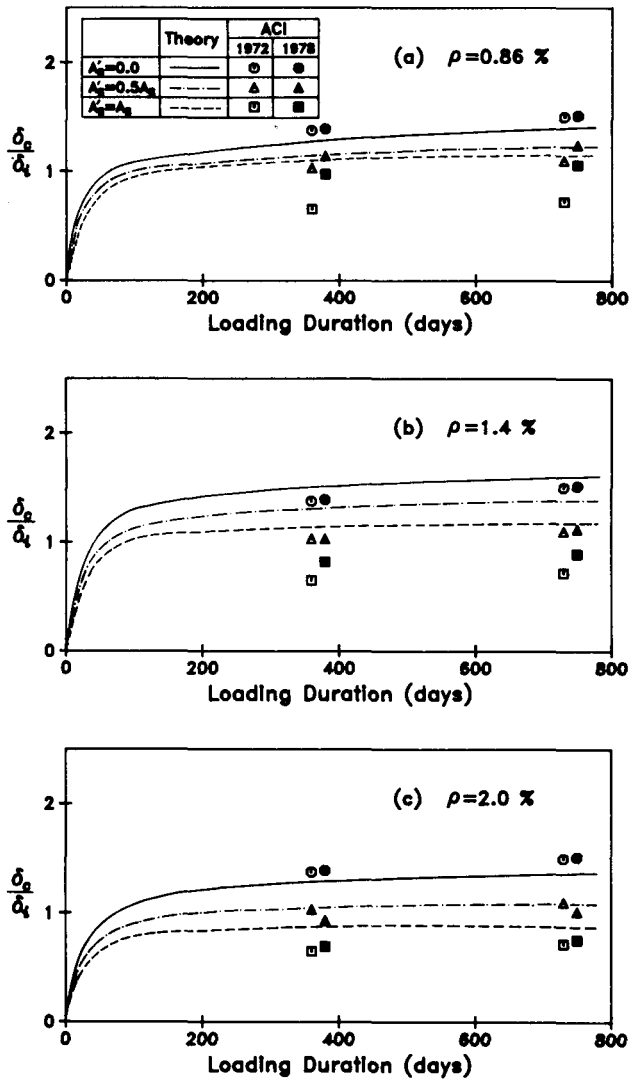


*Fig. 9 — Effect of compression reinforcement $A_s'$ on creep deflection of beams with various tensile reinforcement percentages*

Their parameters are $b = 6$ in., $h = 9$ in., $d = 7.5$ in., $d' = 1.5$ in., $f_c' = 3000$ psi, $f_t' = 274$ psi, $E_c = 3 \times 10^6$ psi, $f_y = 47{,}000$ psi, $E_s = 29 \times 10^6$ psi, and $L = 240$ in. (1 in. = 25.4 mm and 1 psi = 6895 Pa). Fig. 9 exhibits comparisons with the present theory for light, medium, and heavy tensile reinforcements as well as compression reinforcements. Compared to the predictions of the present theory, Eq. (29b), and even more Eq. (29a), generally predict a stronger effect of the compression reinforcements; however, not too much difference is seen in the case of heavy tensile reinforcement. For light tensile reinforcement and equal compression reinforcement the differences are substantial, especially for Eq. (29a). Other investigators[3,27] have commented that Eq. (29a) or (29b) in these cases overestimates the reduction of deflections achieved by compression reinforcement, which is not on the safe side. Thus, our predictions agree with these earlier critical observations.

## Simplified model: Equivalent transformed cross section

Although with a computer (or even a programmable pocket calculator) it is no trouble to carry out the foregoing analysis, hand calculations, albeit feasible, are obviously much more involved than the use of Branson's formula. For hand calculations, it is therefore useful to simplify the model without causing great deviations of results. To make this possible, we restrict the range of applicability to the elastic range of concrete in compression, i.e., the service load range. The only nonlinearity is then caused by the tensile strain-softening.

For this purpose, we neglect the tensile resistance of concrete distributed over the tension side of the neutral axis and seek to determine an equivalent tensile area $A_{eq}$ and an equivalent tensile stress of concrete in this area $f_{eq}$, which would yield about the same beam curvature $\kappa_0$. The centroid of this equivalent area we consider to coincide with that of tensile reinforcement [Fig. 10(a)].

Considering the force equilibrium in the axial direction (at $N = 0$), we have

$$\frac{1}{2}\sigma_1 bkd + f_{s1}A_{s1} - f_{s2}A_{s2} - f_{eq}A_{eq} = 0 \quad (31)$$

in which $\sigma_1$ = stress at the compression face (Fig. 10). Since, in the elastic range

$$f_{s1} = E_s\epsilon_{s1} = \frac{E_s\sigma_1}{E_c}\frac{kd - d_1}{kd}, \quad f_{s2} = E_s\epsilon_{s2} = \frac{E_s\sigma_1}{E_c}\frac{d_2 - kd}{kd}, \quad f_{eq} = \frac{d - kd}{kd}\sigma_1 \quad (32)$$

Eq. (31) yields

$$A_{eq} = \left[\frac{1}{2}b(kd)^2 + nA_s'(kd - d')\right] \times (d - kd)^{-1} - nA_s \quad (33)$$

in which $A_{s1} = A_s'$, $A_{s2} = A_s$, $d_1 = d'$, $d_2 = d$, and $n = E_s/E_c$.

The value of $kd$ needed in Eq. (33) has to be calculated from the condition of the same curvature $\kappa$ [Fig. 10(d) and (e)]. We need to distinguish two cases depending on whether the tensile stress in concrete at the tensile face is zero or finite (Fig. 10).

First assume that the tensile stress $f_1$ at the tensile face is finite [Fig. 10(d)]. Considering the equilibrium condition on zero axial resultant ($N = 0$), we obtain

$$kd = [(r^2 - 4qs)^{1/2} - r](2q)^{-1} \quad \text{for } c_1 + c_2 > h - kd \quad (34)$$

in which

$$q = \frac{1}{2}(1 + m)b(\sigma_1 + 2f_t' + f_t'^2\sigma_1^{-1}),$$

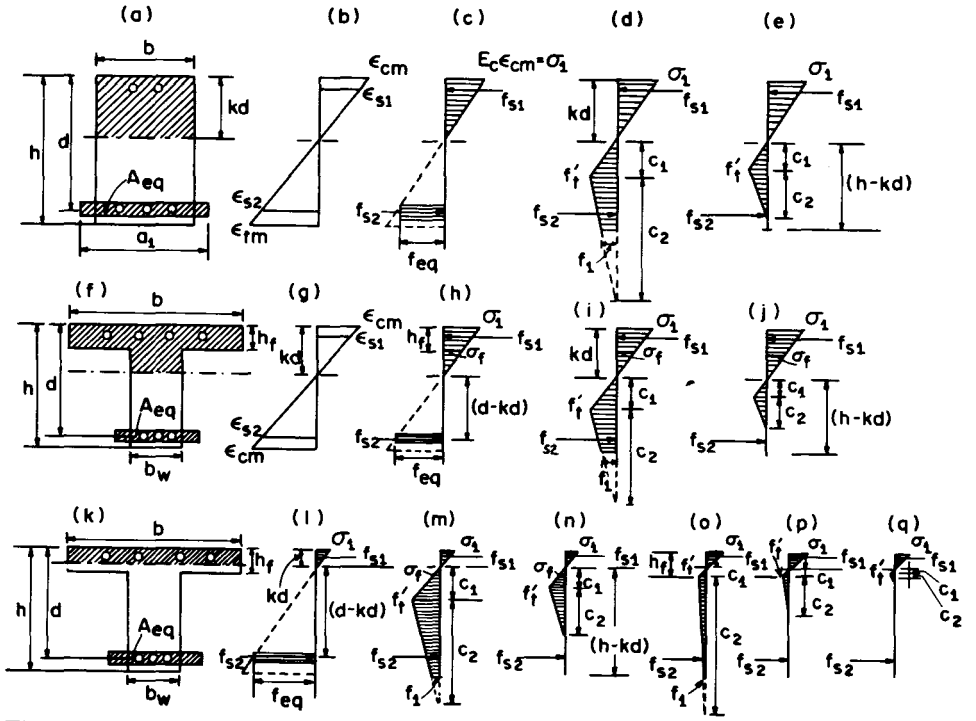


*Fig. 10 — Cross sections considered and stress distributions in various cases and stages*

$$r = n\sigma_1(A'_s + A_s) - bh\,(f'_t + m\sigma_1 + mf'_t)$$

$$s = -n\sigma_1(A'_s d' + A_s d) + \frac{1}{2}bh^2\sigma_1 m$$

$$m = \frac{-E_t}{E_c}, \quad c_1 = \frac{kd}{\sigma_1}f'_t, \quad c_2 = \frac{c_1}{m} \tag{35}$$

Second, if the tensile stress is zero at the tension face [Fig. 10(e)], we have

$$kd = [(r^2 - 4qs)^{1/2} - r]\,(2q)^{-1} \quad \text{for } c_1 + c_2 \leqslant h - kd \tag{36}$$

in which

$$q = \frac{1}{2}b[\sigma_1 - (1 + m^{-1})f'^2_t\sigma_1^{-1}],\ r = n\sigma_1(A'_s + A_s),\ s = -n\sigma_1(A'_s d' + A_s d) \tag{37}$$

Once $kd$ and $A_{eq}$ are determined, the inertia moment of the transformed composite cross section can be easily evaluated. Note that $A_{eq}$ and $kd$ depend on the specified value of $\sigma_1$, and so, strictly speaking, $A_{eq}$ and $kd$ cannot be evaluated for a given bending moment except in an iterative manner. However, for the service stress range one can approximately evaluate $A_{eq}$ and $kd$ assuming $\sigma_1 \simeq 0.3f'_c$. As an approximation, these values of $A_{eq}$ and $kd$ may be considered constant for analysis in the service stress range.

The results of such a simplified analysis are plotted in Fig. 8 as the dashed lines. As seen, the results are essentially as good as those obtained from the original, unsimplified theory. This validates the simplified equivalent area approach for the service stress range.

When the equivalent area approach is used for long-time deflections, the use of an increased creep coefficient in the tensile zone can be conveniently replaced by the use of a transformed equivalent area $A^{tr}_{eq}$

$$A^{tr}_{eq} = A_{eq}\frac{1 + \phi}{1 + \beta_c\phi} \quad (\beta_c \simeq 3) \tag{38}$$

In case of a T-beam, we need to distinguish various further cases depending on the position of the neutral axis, as well as the lines of tensile stress peaks and of the points where the tensile stress is reduced to zero, relative to the bottom of the flange. Consideration of all the possible combinations is rather involved; however, it seems that of main importance is the location of the neutral axis relative to the flange [Fig. 10(f), (h), (k), (l)]. If the neutral axis, as well as the line where the tensile stress is reduced to zero, lies in the flange [Fig. 10(k)], the expression for $A_{eq}$ is the same as that in Eq. (33). If the neutral axis is in the web [Fig. 10(f)], i.e., $kd > h_f$, the equilibrium condition yields

$$A_{eq} = \frac{1}{2}[(2kd - h_f)bh_f + b_w(kd - h_f)^2 + 2nA'_s(kd - d')]\,(d - kd)^{-1} - nA_s \quad (\text{for } kd > h_f) \tag{39}$$

in which $h_f$ = thickness of the flange, and $b_w$ = thickness of the web (Fig. 10). Formulas have also been set up for various locations relative to the flange of the lines of stress peaks and of the points where the tensile

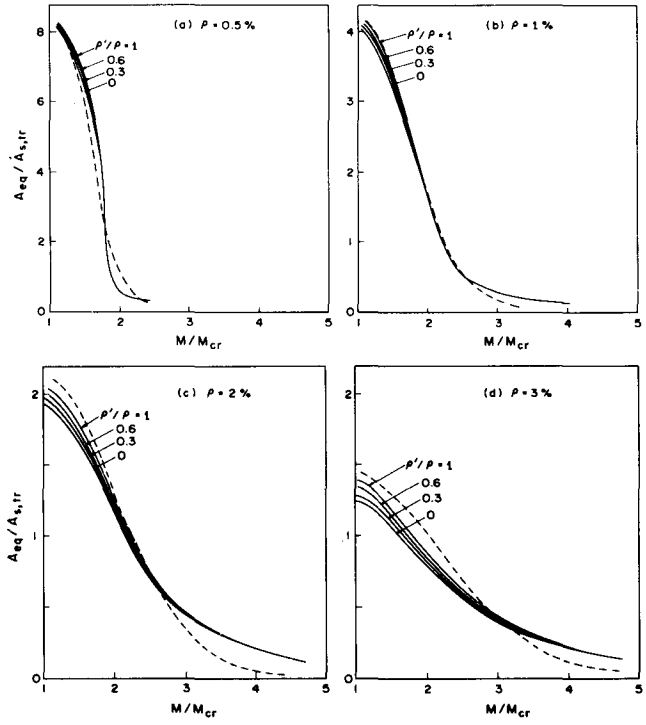


*Fig. 11 — Effect of tensile and compression reinforcement ratios on the equivalent tensile area of concrete (rectangular beam)*

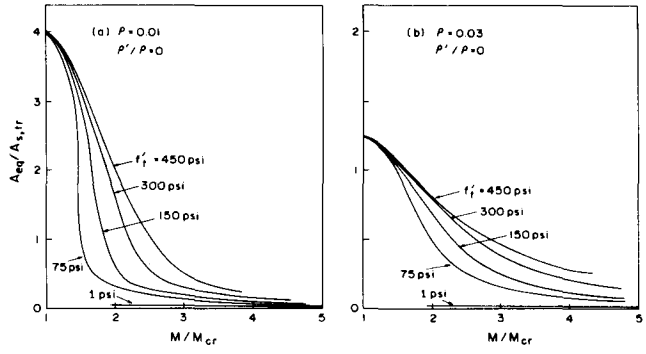


*Fig. 12 — Effect of tensile strength on the equivalent tensile area of concrete (rectangular beam)*

stress is reduced to zero [Fig. 10(i), (j), (m) through (q)]. For the sake of brevity we omit these formulas; however, they can be easily set up from the equivalent condition for the stress diagrams in Fig. 10(i) through (q).

To get a picture of the variation of the exact value of $A_{eq}$ with the bending moment and the percentages of tensile and compression reinforcement, calculations have been made for a typical rectangular cross section, defined by $b$ = 12 in., $h$ = 24 in., $d$ = 21.5 in., $d'$ = 2.5 in., $f'_c$ = 3600 psi, $f'_t$ = 300 psi, $E_c$ = 3420 ksi, $f_y$ = 40 ksi, and $E_s = 29 \times 10^6$ psi (1 in. = 25.4 mm and 1 psi = 6895 Pa). Fig. 11 shows the results, with the notation $A_{s,tr} = nA_s = \rho bdE_s/E_c$ and $M_{cr}$ = cracking moment = $f'_t I_g/y_t$, in which $I_g$ = moment of inertia of the gross cross section and $y_t$ = distance from the neutral axis to the tensile face. These plots show that $A_{eq}$ is almost independent of the ratio of the cross section areas of compression and tensile reinforcement $\rho'/\rho$

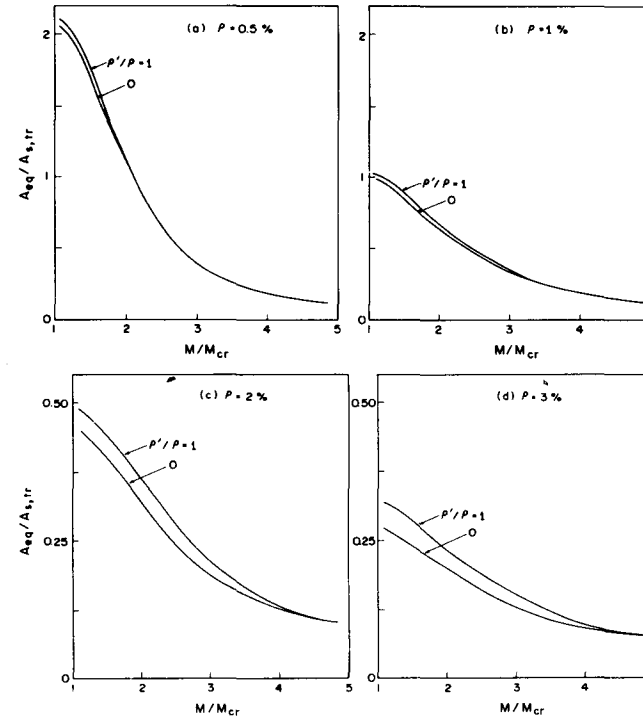


*Fig. 13 — Effect of tensile and compression reinforcement ratios on the equivalent tensile area of concrete in T-beam*

but depends significantly on the percentage of tensile reinforcement and on the bending moment value relative to the cracking moment.

Calculations have further been carried out for various values of the tensile strength $f'_t$; see Fig. 12. This effect seems to be quite significant, not surprisingly, since $A_{eq}$ must vanish for $f'_t \to 0$.

Similar calculations have been carried out for a typical T-beam, defined by the parameters $b$ = 60 in., $b_w$ = 12 in., $h$ = 25 in., $h_f$ = 5 in., $d$ = 22.5 in., $d'$ = 2.5 in., $f'_c$ = 4000 psi, $f'_t$ = 316 psi, $E_c = 3.6 \times 10^6$ psi, $E_s = 29 \times 10^6$ psi, and $f_y$ = 40,000 psi (1 in. = 25.4 mm and 1 psi = 6895 Pa). The results (Fig. 13) indicate similar trends as before.

Finally, it has been studied whether the dependence of $A_{eq}$ on $M$ and $\rho$ (with the dependence on $\rho'/\rho$ being neglected) can be reasonably approximated by some simple formulas. The following formula, plotted as the dashed lines in Fig. 11, has been found

$$A_{eq} \simeq A_{s,tr} \frac{0.043}{\rho} e^{-0.0094\lambda}, \text{ with } \lambda = \frac{1}{\rho}\left(\frac{M}{M_{cr}} - 1\right)^2 \quad (40)$$

The only advantage of the simplified model just outlined over Branson's formula is a broader range of applicability. Certainly, the foregoing definition of $A_{eq}$ can be applied to various cases not covered by this formula.

## CONCLUSIONS

1. The progressive microcracking under increasing loads in reinforced concrete beams subjected to bend-

ing can be taken into account by considering concrete to have a nonzero tensile carrying capacity, described by a tensile stress-strain diagram which includes strain softening. A bilinear tensile stress-strain diagram is sufficient for practical purposes.

2. The tensile stress-strain diagram used here is not determined by fitting curvature and deflection data for beams but is taken to be the same as that obtained in direct tension tests, and also the same as that which provided good representation of various fracture test data for concrete. Correct predictions, which compare well with curvature and deflection test data for reinforced concrete beams, are then obtained by a consistent theoretical analysis for short-time deformations of beams all the way up to the steel yielding range.

3. The theoretical predictions agree well with the well-known formula of Branson within the range for which that formula was developed. Within that range, calculations based on Branson's formula are simpler than those based on present theory.

4. The value of the present theory is that it appears to have a much broader applicability. Aside from applications up to the ultimate load, this is also demonstrated by applying the same theory to longtime creep deformations of concrete beams in flexure. Good agreement with available tests is also obtained. It may be expected that this type of theory based on a tensile stress-softening material behavior could be applied to atypical cross sections, continuous beams and frames, slabs and shells, deep beams and panels, for both short-time and longtime responses.

5. To obtain good agreement with the test data for longtime creep deformations of beams, the creep coefficient for the tensile response including the tensile peak stress region and the strain softening should be considered, on the average, about three times larger than that for creep in compression or small tensile stresses.

6. The theory appears to correctly predict the reduction in creep deflections due to the use of compression reinforcement. The theory predicts a somewhat smaller reduction than an ACI formula for higher steel ratios and a substantially smaller reduction for small steel ratios.

7. The use of the bilinear tensile stress-strain diagram for concrete can be replaced by the use of an equivalent area of tensile concrete centered at the level of reinforcement and behaving linearly. The equivalent area may be determined from the conditions of the same curvature and location of the neutral axis.

8. A considerably simplified model can be obtained by assuming the equivalent tensile area of concrete to be independent of the bending moment and steel ratios. Determining the equivalent area for the mean stress level in the service stress range (about $0.3f'_c$), reasonable deformation predictions are obtained simply by using the transformed cross section method, applied to a cracked cross section which is augmented by the equivalent tensile area that can be evaluated from a formula [Eq. (40)].


## ACKNOWLEDGMENT

Partial financial support under U. S. National Science Foundation Grant No. CEE8003148 to Northwestern University is gratefully acknowledged. Mary Hill is thanked for her superb secretarial assistance.


## REFERENCES


1. ACI Committee 435, "Deflections of Reinforced Concrete Flexural Members," (ACI 435.2R-66)(Reaffirmed 1979), American Concrete Institute, Detroit, 1966, 29 pp.

2. Bažant, Z. P., and Oh, B. H., "Crack Band Theory for Fracture of Concrete," *Materials and Structures/Research and Testing* (RILEM, Paris), V. 16, No. 93, July 1983, pp. 155-177.

3. Branson, Dan E., *Deformation of Concrete Structures,* McGraw-Hill Book Co., New York, 1977, 546 pp.

4. Branson, Dan E., "Design Procedures for Computing Deflections," ACI JOURNAL, *Proceedings* V. 65, No. 9, Sept. 1968, pp. 730-742.

5. Subcommittee 2, ACI Committee 209, "Prediction of Creep, Shrinkage, and Temperature Effects in Concrete Structures," *Designing for Effects of Creep, Shrinkage, Temperature in Concrete Structures,* SP-27, American Concrete Institute, Detroit, 1971, pp. 51-93.

6. Branson, D. E., and Christiason, M. L., "Time-Dependent Concrete Properties Related to Design—Strength and Elastic Properties, Creep, and Shrinkage," *Designing for Effects of Creep, Shrinkage, Temperature in Concrete Structures,* SP-27, American Concrete Institute, Detroit, 1971, pp. 257-277.

7. Park, Robert, and Paulay, Thomas, *Reinforced Concrete Structures,* John Wiley & Sons, New York, 1975, 769 pp.

8. Branson, Dan E., and Trost, Heinrich, "Unified Procedures for Predicting the Deflection and Centroidal Axis Location of Partially Cracked Nonprestressed and Prestressed Concrete Members," ACI JOURNAL, *Proceedings* V. 79, No. 2, Mar.-Apr. 1982, pp. 119-130.

9. Evans, R. H., and Marathe, M. S., "Microcracking and Stress-Strain Curves for Concrete in Tension," *Materials and Structures/Research and Testing* (RILEM, Paris), V. 1, No. 1, Jan.-Feb. 1968, pp. 61-64.

10. Rüsch, H., and Hilsdorf, H., "Deformation Characteristics of Concrete Under Axial Tension," Voruntersuchungen, *Bericht* No. 44, Munich, May 1963.

11. Hughes, B. P., and Chapman, G. P., "The Complete Stress-Strain Curve for Concrete in Direct Tension," *RILEM Bulletin* (Paris), New Series No. 30, Mar. 1966, pp. 95-97.

12. Heilmann, H. G.; Hilsdorf, H. H.; and Finsterwalder, K., "Festigkeit und Verformung von Beton unter Zugspannungen," *Bulletin* No. 203, Deutscher Ausschuss für Stahlbeton, Berlin, 1969, 94 pp.

13. Petersson, P. E., "Crack Growth and Development of Fracture Zone in Plain Concrete and Similar Materials," doctoral dissertation, Lund Institute of Technology, Dec. 1981.

14. Scanlon, A., "Time-Dependent Deflections of Reinforced Concrete Slabs," PhD thesis, University of Alberta, Edmonton, 1971.

15. Lin, Cheng-Shung, and Scordelis, Alexander C., "Nonlinear Analysis of RC Shells of General Form," *Proceedings,* ASCE, V. 101, ST3, Mar. 1975, pp. 523-538.

16. Saenz, Luis P., Discussion of "Equation for the Stress-Strain Curve of Concrete" by Prakash Desayi and S. Krishnan, ACI JOURNAL, *Proceedings* V. 61, No. 9, Sept. 1964, pp. 1229-1235.

17. Sinha, B. P.; Gerstle, Kurt H.; and Tulin, Leonard G., "Response of Singly Reinforced Beams of Cyclic Loading," ACI JOURNAL, *Proceedings* V. 61, No. 8, Aug. 1964, pp. 1021-1038.

18. Agrawal, G. L.; Tulin, Leonard G.; and Gerstle, Kurt H., "Response of Doubly Reinforced Concrete Beams to Cyclic Loading," ACI JOURNAL, *Proceedings* V. 62, No. 7, July 1965, pp. 823-835.

19. Burns, Ned H., and Siess, Chester P., "Plastic Hinging in Reinforced Concrete," *Proceedings,* ASCE, V. 92, ST5, Oct. 1966, pp. 45-64.

20. Burns, Ned H., and Siess, Chester P., "Repeated and Re-

versed Loading in Reinforced Concrete," *Proceedings,* ASCE, V. 92, ST5, Oct. 1966, pp. 65-78.

21. Bažant, Zdeněk P., and Panula, Liisa, "Creep and Shrinkage Characterization for Analyzing Prestressed Concrete Structures," *Journal,* Prestressed Concrete Institute, V. 25, No. 3, May-June 1980, pp. 86-122.

22. Bažant, Z. P., "Mathematical Models for Creep and Shrinkage of Concrete Structures," *Creep and Shrinkage in Concrete Structures,* John Wiley & Sons Limited, Chichester, 1982, pp. 163-255.

23. "Time-Dependent Effects," *Finite Element Analysis of Reinforced Concrete,* American Society of Civil Engineers, New York, 1982, pp. 309-400.

24. Subcommittee 2, ACI Committee 209, "Prediction of Creep, Shrinkage, and Temperature Effects in Concrete Structures," (ACI 209R-82), American Concrete Institute, Detroit, 1982, 108 pp.

25. Bažant, Zdeněk P., and Najjar, Leonard J., "Comparison of Approximate Linear Methods for Concrete Creep," *Proceedings,* ASCE, V. 99, ST9, Sept. 1973, pp. 1851-1874.

26. Neville, A. M., and Dilger, W., *Creep of Concrete: Plain, Reinforced, and Prestressed,* North-Holland Publishing Co., Amsterdam, 1970, 622 pp.

27. Hollington, M. R., "A Series of Long-Term Tests to Investigate the Deflection of a Representative Precast Concrete Floor Component," *Technical Report* No. TRA 442, Cement and Concrete Association, London, 1970, 44 pp.

28. Washa, G. W., and Fluck, P. G., "Effect of Compressive Reinforcement on the Plastic Flow of Reinforced Concrete Beams," ACI JOURNAL, *Proceedings* V. 49, No. 2, Oct. 1952, pp. 89-108.

29. Corley, W. Gene, and Sozen, Mete A., "Time-Dependent Deflections of Reinforced Concrete Beams," ACI JOURNAL, *Proceedings* V. 63, No. 3, Mar. 1966, pp. 373-386.

30. Yu, Wei-Wen, and Winter, George, "Instantaneous and Long-Time Deflections of Reinforced Concrete Beams Under Working Loads," ACI JOURNAL, *Proceedings* V. 57, No. 1, July 1960, pp. 29-50.

31. ACI Committee 435, "Proposed Revisions by Committee 435 to ACI Building Code and Commentary Provisions on Deflections," ACI JOURNAL, *Proceedings* V. 75, No. 6, June 1978, pp. 229-238.

32. Branson, Dan E., "Compression Steel Effect on Long-Time Deflections," ACI JOURNAL, *Proceedings* V. 68, No. 8, Aug. 1971, pp. 555-559.

33. Bažant, Z. P., and Panula, L., "Practical Prediction of Time-Dependent Deformations of Concrete," *Materials and Structures/Research and Testing* (RILEM, Paris), V. 11, No. 65, Sept.-Oct. 1978, pp. 307-328; V. 11, No. 66, Nov.-Dec. 1978, pp. 415-434; and V. 12, No. 69, May-June 1979, pp. 169-183.

34. Bažant, Zdeněk P., and Oh, Byung H., "Deformation of Cracked Net-Reinforced Concrete Walls," *Journal of Structural Engineering,* ASCE, V. 108, No. 1, Jan. 1983, pp. 93-108.

35. Kent, Dudley Charles, and Park, Robert, "Flexural Members with Confined Concrete," *Proceedings,* ASCE, V. 97, ST7, July 1971, pp. 1969-1990.

## APPENDIX — CONCRETE TENSIONS CAUSED BY BOND AND OTHER QUESTIONS

In explanation of the tension-stiffening effect (surveyed, e.g., in Reference 34), consideration is given to the tensile stresses in concrete near the bar, which are transferred into concrete between the cracks by bond stresses. In the planes of continuous cracks, the resultant of such stresses is zero but it is nonzero in the planes between the cracks. The effect of these stresses, i.e., of the stiffness of concrete that adheres to the bar, is to reduce the extension of the bar.

Although this phenomenon surely exists, its importance is hard to assess. Since the local tensile stresses are hardly measurable, indirect logical inferences need to be used. In the present model, this effect is neglected, and the comparisons with experimental evidence or the experimentally verified Branson's formula are satisfactory. However, if the additional stiffening of response due to this effect is very small (say $< 5$ percent), it would not destroy the agreement with test data that has been demonstrated here since the predicted response is slightly softer than the measured one in Fig. 5(a), and partly 5(b), 7(a), and 7(b). We may infer from the experimental comparisons presented here that this effect is probably small. For example, if the equivalent tensile area of concrete around the steel bar, characterizing this effect as an average along the bar length,[34] were about equal to the area of steel $A_s$, the effect would not be very significant compared to that obtained from the preceding analysis which yields equivalent areas of concrete to be 5 to 20 times $A_s$ (Fig. 11). Further investigations of this effect are, however, required.